

The BiomolBiomed publishes an “Advanced Online” manuscript format as a free service to authors in order to expedite the dissemination of scientific findings to the research community as soon as possible after acceptance following peer review and corresponding modification (where appropriate). An “Advanced Online” manuscript is published online prior to copyediting, formatting for publication and author proofreading, but is nonetheless fully citable through its Digital Object Identifier (doi®). Nevertheless, this “Advanced Online” version is NOT the final version of the manuscript. When the final version of this paper is published within a definitive issue of the journal with copyediting, full pagination, etc., the new final version will be accessible through the same doi and this “Advanced Online” version of the paper will disappear.

## RESEARCH ARTICLE

Zhang et al: Gut microbiome in SCI recovery in rats

# Metagenomic and metabolomic analysis of gut microbiome's role in spinal cord injury recovery in rats

Jieqi Zhang<sup>1#</sup>, Xihan Ying<sup>1#</sup>, Rong Hu<sup>1</sup>, Yi Huang<sup>1</sup>, Ruoqi Wang<sup>1</sup>, Lei Wu<sup>1,2</sup>, Dexiong Han<sup>1,2</sup>, Ruijie Ma<sup>1,2\*</sup> and Kelin He<sup>1,2\*</sup>

<sup>1</sup>Key Laboratory of Acupuncture and Neurology of Zhejiang Province, The Third School of Clinical Medicine (School of Rehabilitation Medicine), Zhejiang Chinese Medical University, Hangzhou, China

<sup>2</sup>Department of Acupuncture, The Third Affiliated Hospital of Zhejiang Chinese Medical University, Hangzhou, China

\*Correspondence to Kelin He: [352128492@qq.com](mailto:352128492@qq.com) and Ruijie Ma: [maria7878@sina.com](mailto:maria7878@sina.com).

#Jieqi Zhang and Xihan Ying equally contributed to this work.

DOI: <https://doi.org/10.17305/bb.2025.12164>

---

## ABSTRACT

Spinal cord injury (SCI) induces profound systemic changes, including disruptions in gut microbiome composition and host metabolism. This study aimed to investigate the impact of SCI on gut microbial diversity and serum metabolites in rats, and to explore potential microbiome–metabolite interactions that may influence recovery. Male Sprague-Dawley rats were assigned to either SCI or sham-operated groups. Fecal samples were collected for whole-genome metagenomic sequencing, and serum samples were analyzed using untargeted metabolomics. Gut microbial composition and diversity were assessed using  $\alpha$ - and  $\beta$ -diversity indices, while Linear discriminant analysis Effect Size (LEfSe) identified differentially abundant taxa. Metabolomic pathway analysis was performed to detect significant changes in serum metabolites, and Spearman’s correlation was used to evaluate associations between gut microbes and metabolites. SCI significantly altered gut microbiota composition, with increased proportions of *Ligilactobacillus* and *Staphylococcus*, and decreased proportions of *Lactobacillus* and *Limosilactobacillus*. Metabolomic analysis revealed disrupted energy metabolism and elevated oxidative stress in SCI rats, as indicated by increased serum levels of pyruvate and lactic acid. Correlation analysis further identified significant associations between specific gut bacteria and key metabolites, suggesting microbiome-driven metabolic dysregulation following SCI. These findings highlight significant interactions between the gut microbiota and host metabolism after SCI and suggest that microbiome-targeted interventions may hold therapeutic potential for improving recovery by modulating metabolic function and oxidative stress responses.

**Keywords:** Spinal cord injury; SCI; metagenomics; metabolomics; gut microbiome

## INTRODUCTION

Spinal cord injury (SCI) is a devastating neurological condition that imposes significant psychological and economic burden on patients and their families. Over the past 30 years, the global incidence of SCI has been increasing, with an estimated annual incidence of 25,000–50,000 worldwide [1]. SCI leads to the loss of motor, sensory, and autonomic functions and triggers a series of complex systemic disorders including, but not limited to, cardiovascular, respiratory, urinary, and gastrointestinal dysfunctions [2–4]. These systemic effects further complicate the rehabilitation of patients with SCI and increase the treatment challenges.

Recent developments in microbiome research have underscored the significant role of gut microbial communities in human health [5–7]. The loss of central nervous system (CNS)

---

control over the digestive system can lead to significant changes in the gut microbiome [8,9], which are closely associated with the recovery process and development of systemic diseases following SCI(10). Moreover, alterations in the gut microbiome can retroactively affect the host, further complicating the biological impact of SCI [11]. These phenomena are not only closely related to SCI but have also been observed in other CNS disorders. For instance, studies on patients with traumatic brain injury (TBI) have found that changes in the gut microbiome are associated with TBI neuroinflammation, cognitive decline, and behavioral issues [12]. Similarly, research on neurodegenerative diseases such as Alzheimer's disease has shown that imbalances in the gut microbiome may be linked to the progression of these diseases [13]. These findings highlight a complex and profound interaction between the gut microbiome and CNS, suggesting that modulating this interaction could offer new strategies for treating or alleviating these conditions.

In this study, we used SCI rat models to conduct a comprehensive analysis of stool and serum samples from 14-day SCI model rats and sham operation rats using fecal metagenomic shotgun sequencing and serum non-targeted metabolome techniques. Our research aimed to assess the structural and functional changes in the gut microbiome following SCI and explore the potential associations between these changes and the metabolic state of the host. We hypothesized that, compared to the sham group, SCI model rats would exhibit significant alterations in their gut microbiome composition, which could be closely related to changes in the host's metabolic state. Through this study, we hope to deepen our understanding of the complex interactions underlying the effects of SCI and provide new insights into common changes in the gut microbiome associated with human CNS diseases, such as TBI and Alzheimer's disease.

## **MATERIALS AND METHODS**

### **Animals**

Due to the higher prevalence of SCI in male patients in clinical settings, we used male Sprague-Dawley (SD) rats in this study. Healthy adult male SD rats (8 weeks old, weighing 200-220 grams) were obtained from Shanghai Xipu Bikai Experimental Animal Company (animal license No. SCXK(Shanghai)2018-0006) and housed at the Laboratory Animal Center of Zhejiang Chinese Medical University, which is accredited by the Association for Assessment and Accreditation of Laboratory Animal Care (AAALAC; animal license No. SYXK (Zhejiang) 2018-0012). The rats were maintained under controlled conditions with free access

---

to food and water. To ensure equal access to food and water, baskets containing food and water were placed at a lower height in the cages, and both food and water were provided in sufficient quantities and monitored daily to ensure that all rats could access them equally. At the end of the experiment, the animals were euthanized by an overdose of anesthesia in accordance with ethical guidelines.

In this study, we used male rats exclusively to minimize the variability caused by hormonal fluctuations, as estrogen levels in female rats could significantly affect gut microbiome composition and metabolic profiles. A total of 16 rats were randomly assigned to either the SCI group (8 rats) or the sham group (8 rats), with four rats housed per cage. All animal experiments were conducted in accordance with the protocol approved by the Animal Ethics Committee of Zhejiang Chinese Medical University (I ACUC-20230313-01) and strictly followed the National Institutes of Health (NIH) guidelines for the use of experimental animals (NIH Publication No. 8023).

### **SCI model**

Rats were anesthetized via intraperitoneal injection of sodium pentobarbital (30 mg/kg) and operated on a constant-temperature surgical table. After exposing the T10 spinal cord through surgery, the NYU impactor SCI system was used to deliver a precise blow to the spinal cord under computer control, creating the rat SCI model, which weighed 10 g \* 5 cm potential energy impact centered on the T10 segment of the spinal cord, causing moderate injury to the T10 segment. The skin was sutured after cleaning. Successful model preparation included possible spasmodic twitching, tail-flicking, dural congestion, or hematoma. Rats waking up with a BBB (Basso, Beattie, Bresnahan) score of 0-2 were considered to be successfully modelled [14]. In the sham group, the vertebral plate was removed to expose the spinal cord, without any impact applied to the spinal cord. Postoperative care for all animals, including both the sham and SCI groups, included intraperitoneal injections of penicillin (100 U / day) for the first three days. Additionally, the rats in the model group received twice-daily abdominal massages to assist urination until they could urinate autonomously.

### **Sample collection and preparation**

14 days after the SCI model was established each rat was placed in a separate sterile cage. At least two fecal pellets were collected from each rat, placed in sterile conical tubes, and rapidly frozen in liquid nitrogen before being stored at -80°C for further microbiome analysis. At the

---

end of the experiment, blood was collected under anesthesia with sodium pentobarbital via the abdominal aorta. Serum was isolated and stored at -80°C.

### **Metagenome DNA extraction and shotgun sequencing**

Microbial DNA from all samples was isolated with the OMEGA Mag-Bind Soil DNA Kit (M5635-02) (Omega Bio-Tek, Norcross, GA, USA), according to the provided guidelines, and then kept at -20°C for future analysis. The amount and purity of isolated DNAs were assessed utilizing a Qubit™ 4 Fluorometer, equipped with WiFi Q33238 (Qubit™ Assay Tubes Q32856; Qubit™ 1X dsDNA HS Assay Kit Q33231) (Invitrogen, USA) and agarose gel electrophoresis, respectively. Microbial DNA was extracted and then used to create metagenome shotgun sequencing libraries with 400 bp insert sizes, utilizing the Illumina TruSeq Nano DNA LT Library Preparation Kit. Metabo-Profile Biotechnology Co., Ltd. in Shanghai, China utilized the Illumina NovaSeq platform from Illumina, USA to sequence every library using the PE150 strategy.

The complete microbial genomic DNA was isolated with the OMEGA Mag-Bind Soil DNA Kit (M5635-02) from Omega Bio-Tek in Norcross, GA, USA, following the provided guidelines, and then kept at -20°C for future analysis. DNA amount and purity were assessed with the Qubit™4 Fluorometer, WiFi Q33238 (Qubit™ Assay Tubes Q32856; Qubit™1X dsDNA HS Assay Kit Q33231) from Invitrogen, USA, as well as agarose gel electrophoresis. The Illumina TruSeq Nano DNA LT Library Preparation Kit was utilized for processing the isolated microbial DNA to create metagenomic shotgun sequencing libraries with an insert size of 400 bp. The Illumina NovaSeq platform (Illumina, USA) and metabo-profile Biotechnology Co., Ltd. (Shanghai, China) PE150 strategy were used to sequence every library.

### **Metagenomics analysis**

Raw sequencing reads were filtered for quality and classified using Kraken2 against the RefSeq-derived database. Samples were assembled using Megahit, and contigs longer than 300 bp were clustered using mmseqs2. Only relevant contigs were retained by aligning them against the NCBI-nt database to identify and exclude non-target taxonomy. Gene prediction was performed using MetaGeneMark software. Gene abundance was quantified by mapping reads to these sequences using Salmon, and the results were normalized by CPM. Functional annotations of genes were carried out against the KEGG, EggNOG, and CAZy databases using

---

mmseqs2. Additional annotations were performed using EggNOG-mapper and KOBAS to obtain enriched biological insights.

### **Serum extraction and metabolomics analysis**

Chemicals for targeted metabolites were sourced from Sigma-Aldrich, Steraloids Inc., and TRC Chemicals and were prepared in relevant solvents to prepare stock solutions. Sample preparation involved thawing plasma on ice, adding it to wells, and processing with methanol and internal standards using an Eppendorf epMotion Workstation, followed by centrifugation and derivatization. The analysis was performed using the ACQUITY UPLC-Xevo TQ-S system (Waters Corp.) and the UPLC BEH C18 column (1.7  $\mu\text{m}$ , 2.1  $\times$  100 mm) with a VanGuard pre-column (1.7  $\mu\text{m}$ , 2.1  $\times$  5 mm). The mobile phase consisted of A: Water with 0.1% formic acid, and B: Acetonitrile/isopropanol (70:30). The gradient conditions were as follows: 0-1 min (5% B), 1-11 min (5-78% B), 11-13.5 min (78-95% B), 13.5-14 min (95-100% B), 14-16 min (100% B), 16-16.1 min (100-5% B), 16.1-18 min (5% B). The flow rate was set at 0.40 mL/min, and the column temperature was maintained at 40°C. The injection volume was 5  $\mu\text{l}$ . Quality control included the use of internal standards and pooled QC samples to ensure consistency and reliability of the data. Data from UPLC-MS/MS were analyzed using the TMBQ software for peak integration and quantitation, and statistical analysis was performed to interpret the metabolic data.

### **Ethical statement**

Ethical approval was obtained from the Animal Ethics Committee of Zhejiang Chinese Medical University (I ACUC-20230313-01).

### **Statistical analysis**

Statistical analyses and data visualization were performed using R software (version 4.1.2). Descriptive statistics, such as means and standard deviations for continuous variables and frequencies and percentages for categorical variables, were calculated. Group comparisons were conducted using t-tests for continuous variables and chi-squared tests for categorical variables.  $\beta$ -Diversity analysis was performed using the Bray-Curtis distance and visualized by principal coordinate analysis (PCoA). MaAsLin2 was used to identify the differentially enriched taxa and their functions. Metabolomic data were analyzed using Orthogonal Partial Least Squares Discriminant Analysis (OPLS-DA) and univariate tests (t-test, Mann-Whitney U test). Multiple testing corrections were applied, as needed. Statistical significance was set at  $P < 0.05$ .

---

## RESULTS

### SCI induces significant changes in gut microbial composition and diversity

To investigate the changes in intestinal microbiome composition and diversity of SCI rats, this study employed whole-genome shotgun sequencing of fecal samples to compare the gut microbiome between the sham and SCI groups. The experimental timeline outlines key procedures, including establishment of the SCI model, BBB test, and sample collection (Figure 1A). Recovery was assessed over 14 days by using the BBB test. On the first day after surgery, all SCI group rats had a BBB score of 0, which gradually increased over time. In contrast, the sham group maintained a BBB score of 21 throughout the study (Figure 1B). We then drew a cladogram illustrating the overall species composition, diversity, and abundance distribution (Figure 1C). At the genus level, stacked columns of the top 20 dominant species showed an increased proportion of *ligilactobacillus* and *Staphylococcus* in the SCI group, whereas the proportions of *Lactobacillus* and *Limosilactobacillus* decreased (Figure 1D). The  $\alpha$ -diversity analysis revealed significant increases in the Chao1 and ACE indices in the SCI group, suggesting that SCI may promote the richness of rare or undetected species (Figure 1E).  $\beta$ -Diversity analysis using PCoA plots showed clear clustering separation between the SCI group and the sham group, with ANOSIM analysis giving an R-value of 0.5625 and a p-value <0.05, and significant differences in microbial composition between the two groups were confirmed (Figure 1F).

### Key differences in gut microbial community structure following SCI

Further MaAsLin2 analysis revealed significant differences in key genera between the SCI group and the sham group, with the coefficients reflecting the changes in the relative abundance of microbiota in the SCI group compared to the sham group. A bidirectional bar chart was generated to represent the coefficients (coef) of key genera with significant changes in the SCI group (Figure 2A).

These differences in microbial composition were further illustrated using box plots (Figure 2B-M). The data from these plots confirmed significant differences in microbial composition. Specifically, *Corynebacterium*, *Macrococcus*, *Mammaliicoccus*, *Oligella*, and *Jeotgalicoccus* were more abundant in the SCI group. In contrast, genera such as *Lactococcus*, *Limosilactobacillus*, *Romboutsia*, and *Lactobacillus* were significantly reduced in the SCI group compared to the sham group, suggesting that SCI leads to a shift in the gut microbiome composition, with an increase in potentially immune-modulating or inflammation-related

---

genera and a decrease in genera that are typically associated with gut health and barrier function.

### **Impact of SCI on functional features of gut microbiome**

Using databases, such as KEGG metabolic pathways, eggNOG functional categories, CAZy enzyme families, and GO functional groups, we evaluated the functional characteristics of the gut microbiome in rats with sham and SCI. We found that carbohydrate, amino acid, lipid, and energy metabolism were the key metabolic pathways that were significantly enriched in KEGG metabolic pathway analysis (Figure 3). GO analysis revealed enrichment in the metabolic process category under biological processes (BP) and antioxidant activity under molecular functions (MF) (Figure 4). Analysis of the CAZy database showed enrichment of Glycoside Hydrolases (GHs), Glycosyl Transferases (GT), and (carbohydrate-binding module Carbohydrate-Binding Module (CBM) families among the gut microbiome (Figure 5A). EggNOG analysis highlighted the potential impact of the gut microbiome on carbohydrate metabolism (Figure 5B). These findings suggest possible roles of the gut microbiome in host metabolism and the oxidative stress response in SCI.

### **Functional differences in gut microbiome following SCI**

Next, we compared the functional profiles of the gut microbiota between the SCI and sham groups to identify the effects of SCI on the intestinal microbial function. First, we performed principal coordinate analysis (PCoA) and ANOSIM analyses. The results showed that while the KEGG Orthology (KO) analysis did not reveal significant functional differences ( $R = 0.0614$ ,  $P = 0.174$ ) (Figure 6A), the eggNOG analysis showed a slight but statistically significant difference between the two groups ( $R = 0.1395$ ,  $P < 0.05$ ), indicating weak inter-group functional variation (Figure 6B). Subsequently, we used the MaAsLin2 package for further analysis. Heatmaps and dot plots were generated to represent top 20 most significant pathways (based on coef values) to identify the functional pathways affected by SCI. Only pathways with  $FDR < 0.05$ , excluding the “unknown” category, were considered (Figure 6C). Focusing on the “Metabolism” category, we identified several significantly enriched pathways, including secondary metabolite biosynthesis, lipid transport, and energy production and conversion. These findings suggest that SCI-induced changes in the gut microbiota may lead to alterations in metabolic processes, potentially influencing energy metabolism and lipid biosynthesis, which could be critical for understanding the pathophysiological effects of SCI.

---

## Significant changes in host serum metabolites due to SCI

To explore the interaction between changes in the gut microbiome composition and host metabolism, we performed an untargeted metabolomic analysis of the host serum. The distribution of all sample metabolites by category is presented in a pie chart (Figure 7A), which reveals the relative proportions of the main components in the metabolite combination. The results indicated that carbohydrates (38.67%) and organic acids (33.43%) were the predominant metabolites in the serum, followed by amino acids (23.39%). Fatty acids (2.08%) and other categories (2.42%) were present in lower proportions.

OPLS-DA further revealed clear differences in metabolic features between the two groups, with score plots (Figure 7B) and model permutation test results, which verified the validity of the OPLS-DA model (Figure 7C). Based on the OPLS-DA model, we identified metabolites that significantly contributed to group differences by examining both the contribution of these metabolites to the model grouping (VIP, Variable Importance in Projection) and their reliability (Corr. Coefficients and correlation coefficients with the first principal component), with VIP > 1 considered significant differential metabolites.

Further univariate testing identified 27 significantly different metabolites between the two groups, which we presented in a volcano plot (Figure 7D), derived entirely from the metabolite set with a VIP > 1 based on OPLS-DA. A Z-score plot (Figure 7E) specifically displays the standardized expression differences of these metabolites, providing a visual comparison.

The analysis results showed that increases in pyruvic acid and lactic acid in the SCI group indicated disordered energy metabolism and local tissue hypoxia. A decrease in carnosine levels reflects increased oxidative stress in SCI patients. Elevated aspartic acid levels may be related to changes in neurotransmitter activity. A reduction in 3-Hydroxyisovaleric acid represented changes in fatty acid metabolism pathways, possibly related to energy production and inflammatory responses.

We also conducted a pathway analysis of these 27 metabolites using the rno library (Figure 7F), enriching eight pathways ( $p < 0.05$ ). These pathways are primarily involved in energy metabolism, amino acid metabolism, and pathways related to inflammation and nerve repair. Key processes include the citrate cycle (TCA cycle); biosynthesis and degradation of branched-chain amino acids such as valine, leucine, and isoleucine; metabolism of amino acids such as alanine, aspartate, and glutamate; and the metabolism of arginine and proline. Other important pathways included histidine, butyrate, and propionate metabolism.

---

In summary, the metabolic changes induced by SCI encompass disordered energy metabolism, increased oxidative stress, changes in neurotransmitter activity, and metabolic pathway alterations, providing important information for understanding the biological basis of SCI and developing treatment strategies.

### **Potential links between gut microbiome and serum metabolites in SCI**

Finally, we employed Spearman's correlation analysis to explore the relationships between the gut microbiome and serum metabolites, with the results displayed in a heatmap (Figure 8). Notably, *Limosilactobacillus* showed a positive correlation with Carnosine and 3-Hydroxyisovaleric acid, both related to the synthesis and degradation of amino acids; *Lactococcus* was positively correlated with isocitric acid, which is important in energy metabolism; and *Romboutsia* was positively correlated with short-chain fatty acid metabolism-related isobutyric acid and ethylmethylacetic acid. These findings emphasize the complex interactions between the gut microbiome and host metabolites and provide new insights into the mechanisms underlying the impact of SCI on the host.

## **DISCUSSION**

Our study systematically revealed profound changes in the composition and function of the gut microbial community and its interactions with host metabolism in SD rats 14 d after SCI. Our results show that SCI causes significant changes in gut microbiome composition, particularly the increased proportions of *Ligilactobacillus* and decreased proportions of *Lactobacillus* and *Limosilactobacillus*. This is similar to the findings of other scholars, who have noted significant changes in gut microbiota SCI, particularly reductions in populations of anti-inflammatory bacteria such as *Lactobacillus* [15]. Furthermore, the results of species  $\alpha$ -diversity and  $\beta$ -diversity analyses further confirmed that the gut microbiome underwent significant changes in diversity and structure after SCI. These changes may reflect the impact of gastrointestinal environmental alterations on microbial community structure after SCI.

Additionally, our species  $\alpha$ -diversity index analysis revealed increases in the Chao1 and ACE indices, indicating an increase in rare or undetected species, contrary to the findings of Jing et al.[16]. Jing et al. used a C57 mouse model and collected samples at 4 weeks post-injury, whereas our study was based on an SD rat model with sample collection at 14 days post-injury. These differences may account for the inconsistencies observed.[17]. Although no significant differences were observed in the Shannon and Simpson indices, these two diversity indices exhibited higher stability in the sham group, whereas significant increases in within-group

---

variability in the SCI group may indicate a decrease in the stability of the gut microbiome[18]. Species  $\beta$ -diversity analysis further confirmed the significant changes in the gut microbiome composition induced by SCI, which may vary widely among individuals in the SCI group.

Further MaAsLin2 analysis revealed significant differences in key species under SCI conditions, revealing complex interactions between the gut microbiota that are essential for understanding the role of gut microbiota in SCI recovery. The decreased abundance of *Limosilactobacillus* and *Lactococcus*, both producers of beneficial metabolites, such as lactate, might impair mucosal health and immune modulation[19,20]. *Limosilactobacillus* can also salvage cognitive functions associated with dysplasia and dysfunction of the blood-brain barrier[21]. *Romboutsia* is significantly reduced after SCI and its role appears to be dual. It is an important producer of short-chain fatty acids (SCFAs) and contributes to gut health and immune regulation[22,23]. However, under specific stress conditions, overactivity may exhibit proinflammatory properties and disrupt host metabolic homeostasis[24].

Conversely, our findings also underscore the detrimental effects of certain pathogens on gut microbiota composition. For instance, *Corynebacterium* and *Macrooccus* are upregulated in the SCI group, which may be associated with enhanced neuroinflammation and oxidative stress, potentially exacerbating neuronal damage[25–27]. However, some probiotics, such as *Ligilactobacillus*, were also enriched. *Ligilactobacillus* has been shown to alleviate anxiety and depression-like disorders in mice with chronic unpredictable mild stress by regulating tryptophan metabolism. In our study, most pathogens or opportunistic pathogens were present at higher levels in the SCI group, further supporting the hypothesis that the gut microbiota may influence recovery following SCI.

Specifically, our analysis of the functional composition of the gut microbiome identified significant enrichment of key metabolic pathways related to energy metabolism, inflammatory response, and nerve repair, emphasizing the potential effect of the gut microbiota on spinal cord injury recovery [28–31]. Functional  $\beta$ -diversity analysis revealed subtle differences between the two groups, suggesting that the functional profiles of the microbial communities were largely similar at the macro-level. However, MaAsLin2 analysis of eggNOG-enriched pathways identified differential pathways that were mainly related to secondary metabolite biosynthesis, carbohydrate metabolism, energy production, lipid metabolism, and amino acid metabolism[32].

---

The upregulation of secondary metabolite biosynthesis pathways suggests increased microbial stress responses, potentially involving the production of anti-inflammatory or proinflammatory compounds[33]. The enriched pathways related to carbohydrate and lipid metabolism suggest that carbohydrate intolerance and lipid abnormalities commonly observed after SCI may be linked to gut microbiota dysbiosis[34]. The upregulation of energy metabolism pathways indicates increased energy demand by the host, which may represent a compensatory response to the altered physiological state following SCI[35]. Moreover, changes in amino acid transport and metabolism highlight the potential disruptions in neurotransmitter synthesis, immune regulation, and tissue repair processes[36,37].

In metabolomics analysis, the increase in serum metabolites, such as pyruvate and lactic acid, may reflect disordered energy metabolism and a state of local tissue hypoxia in SCI[38]. Additionally, a decrease in carnosine levels highlights the increase in oxidative stress in SCI, which may exacerbate damage to nerve cells[39]. We further explored the changes in serum metabolic pathways in SCI through rno pathway analysis, identifying significant changes in pathways involved in energy metabolism, amino acid metabolism, and pathways related to inflammation and nerve repair. These findings not only provide important clues for understanding the biological basis of SCI but also offer valuable information for developing new diagnostic markers, assessing the severity of SCI, and designing treatment strategies. It is worth noting that the changes in intestinal microbial community function after SCI were correlated with the different analysis results of serum metabolites. This finding strengthens the close link between the gut microbiome and host metabolism, particularly in areas with disordered energy metabolism, increased oxidative stress, and changes in neurotransmitter activity.

Finally, our correlation analysis demonstrated significant links between the gut microbiome and serum metabolites, suggesting potential relationships between certain bacterial genera and metabolites. For example, the positive correlation between *Limosilactobacillus* and carnosine may indicate a potential role of this genus in alleviating oxidative stress in SCI patients. Additionally, *Limosilactobacillus* influences the levels of creatine, pyruvic acid, and lactic acid by degrading nitrite [40–42]. These interactions suggest that the gut microbiome can significantly affect the health and recovery process of the host following SCI by modulating the production and regulation of critical metabolites[43,44]. *Limosilactobacillus* is one of the most extensively studied strains in clinical research[45]. Specifically, *L. reuteri* has demonstrated certain effects in improving symptoms of hyperactivity and social skills, as well

---

as in enhancing mental states related to anxiety and depression in humans[46,47]. While *Lactococcus* has not yet been widely reported for its clinical application in oral medications, its potential as a probiotic is being actively explored. For instance, *L. lactis* has been shown to prevent experimental autoimmune encephalomyelitis in mice[48]. Moreover, *L. lactis* can produce GABA through its metabolism, thereby modulating the gut-brain axis[49,50]. This provides new insights into how gut microbiota can regulate central nervous system disorders. Taken together, our findings highlight the significant impact of the gut microbiome on host metabolism. By altering metabolite levels, the gut microbiome not only influences immediate biochemical pathways but also plays a crucial role in the overall health outcomes and recovery mechanisms of the host. This insight into the metabolic functions of the gut microbiota opens new avenues for targeted therapeutic strategies that harness the potential of the microbiome to enhance host metabolic health and recovery.

In this study, metagenomics and metabolomics were combined to investigate the effects of SCI on the intestinal microbiome and host metabolism of rats. Our study provides important insights into the potential effect of the gut microbiome on SCI recovery and points to therapeutic strategies and development potential for gut microbiome-based intervention in SCI. Here, we provide a comprehensive summary of the strengths and limitations of our study: 1) Our study combined metagenomics and metabolomics approaches to analyze the effects of SCI on the gut microbiome and host metabolism, presenting a panoramic view of the gut microbiome to host functional effects. 2) Through a detailed analysis of the composition of the gut microbiome and host serum metabolites, we revealed significant changes in the structure and function of the gut microbiome and host metabolites in SCI, suggesting potential involvement of the gut microbiome in influencing host responses to oxidative stress and energy metabolism, providing a broader perspective for understanding the complex mechanisms of SCI. 3) Our findings highlight the potential of gut microbiome interventions as a new strategy for treating SCI, providing a scientific basis for developing new treatment methods. 4) While we identified an association between the gut microbiome and serum metabolism, the mechanisms by which these changes specifically affect the SCI recovery process have not been fully addressed in this study. 5) Although the study results support the development of treatment strategies based on the gut microbiome, their practical application in clinical treatment is still in the early stages, and the specific intervention methods and effects require further research and exploration [51,52]. Future studies will further validate the relationship

---

between gut microbiota and host metabolites following spinal cord injury through fecal microbiota transplantation and supplementation of those metabolites.

## CONCLUSION

In this study, metagenomic and serum metabolomic methods were used to provide a unique perspective and new insights for understanding gut microbiome changes and their impact on host health after SCI. Despite these limitations, our findings highlight the potential influence of the gut microbiome on SCI recovery, providing a scientific basis for exploring new therapeutic directions in the future. The specific mechanisms linking the gut microbiome and recovery from SCI need to be further explored to evaluate the effectiveness and safety of therapeutic strategies based on these findings.

**Conflicts of interest:** Authors declare no conflicts of interest.

**Funding:** This work was supported by the National Natural Science Foundation of China (nos. 82205258, 82174487 and 82205282), the Postdoctoral Fellowship Program of CPSF (nos. GZB20240217) and Zhejiang Chinese Medical University Research Fund (nos. 2022FSYYZZ08 and 2022FSYYZY09).

**Data availability:** Raw data generated during the current study were deposited in the Zenodo repository. Data can be accessed using the following DOI: 10.5281/zenodo.12696988.

**Submitted:** 07 February 2025

**Accepted:** 18 March 2025

**Published online:** 26 March 2025

## REFERENCES

1. Khorasanizadeh M, Yousefifard M, Eskian M, Lu Y, Chalangari M, Harrop JS, et al. Neurological recovery following traumatic spinal cord injury: a systematic review and meta-analysis. *Journal of Neurosurgery: Spine*. 2019 May;30(5):683–99.
2. Sun X, Jones ZB, Chen X ming, Zhou L, So KF, Ren Y. Multiple organ dysfunction and systemic inflammation after spinal cord injury: a complex relationship. *J Neuroinflammation*. 2016 Dec;13(1):260.
3. Williams AM, Gee CM, Voss C, West CR. Cardiac consequences of spinal cord injury: systematic review and meta-analysis. *Heart*. 2019 Feb;105(3):217–25.

- 
4. Lefèvre C, Bessard A, Aubert P, Joussain C, Giuliano F, Behr-Roussel D, et al. Enteric Nervous System Remodeling in a Rat Model of Spinal Cord Injury: A Pilot Study. *Neurotrauma Reports*. 2020 Oct 1;1(1):125–36.
  5. Fan Y, Pedersen O. Gut microbiota in human metabolic health and disease. *Nat Rev Microbiol*. 2021 Jan;19(1):55–71.
  6. Sorboni SG, Moghaddam HS, Jafarzadeh-Esfehani R, Soleimanpour S. A Comprehensive Review on the Role of the Gut Microbiome in Human Neurological Disorders. *Clin Microbiol Rev*. 2022 Jan 19;35(1):e00338-20.
  7. De Vos WM, Tilg H, Van Hul M, Cani PD. Gut microbiome and health: mechanistic insights. *Gut*. 2022 May;71(5):1020–32.
  8. Yuan B, Lu X jie, Wu Q. Gut Microbiota and Acute Central Nervous System Injury: A New Target for Therapeutic Intervention. *Front Immunol*. 2021 Dec 24;12:800796.
  9. Liu L, Huh JR, Shah K. Microbiota and the gut-brain-axis: Implications for new therapeutic design in the CNS. *eBioMedicine*. 2022 Mar;77:103908.
  10. Jogia T, Ruitenber MJ. Traumatic Spinal Cord Injury and the Gut Microbiota: Current Insights and Future Challenges. *Front Immunol*. 2020 May 8;11:704.
  11. Cui Y, Liu J, Lei X, Liu S, Chen H, Wei Z, et al. Dual-directional regulation of spinal cord injury and the gut microbiota. *Neural Regeneration Research*. 2024 Mar;19(3):548–56.
  12. Rice MW, Pandya JD, Shear DA. Gut Microbiota as a Therapeutic Target to Ameliorate the Biochemical, Neuroanatomical, and Behavioral Effects of Traumatic Brain Injuries. *Front Neurol*. 2019 Aug 16;10:875.
  13. Chen C, Liao J, Xia Y, Liu X, Jones R, Haran J, et al. Gut microbiota regulate Alzheimer’s disease pathologies and cognitive disorders via PUFA-associated neuroinflammation. *Gut*. 2022 Nov;71(11):2233–52.
  14. Wei Z, Wang Y, Zhao W, Schachner M. Electro-Acupuncture Modulates L1 Adhesion Molecule Expression After Mouse Spinal Cord Injury. *Am J Chin Med*. 2017;45(1):37–52.
  15. Kigerl KA, Hall JCE, Wang L, Mo X, Yu Z, Popovich PG. Gut dysbiosis impairs recovery after spinal cord injury. *Journal of Experimental Medicine*. 2016 Nov 14;213(12):2603–20.
  16. Jing Y, Yu Y, Bai F, Wang L, Yang D, Zhang C, et al. Effect of fecal microbiota transplantation on neurological restoration in a spinal cord injury mouse model: involvement of brain-gut axis. *Microbiome*. 2021 Mar 7;9(1):59.
  17. Bannerman CA, Douchant K, Segal JP, Knezic M, Mack AE, Lundell-Creagh C, et al. Spinal cord injury in mice affects central and peripheral pathology in a severity-dependent manner. *Pain*. 2022 Jun 1;163(6):1172–85.

- 
18. Kim BR, Shin J, Guevarra RB, Lee JH, Kim DW, Seol KH, et al. Deciphering Diversity Indices for a Better Understanding of Microbial Communities. *Journal of Microbiology and Biotechnology*. 2017 Dec 28;27(12):2089–93.
  19. Cervantes-García D, Jiménez M, Rivas-Santiago CE, Gallegos-Alcalá P, Hernández-Mercado A, Santoyo-Payán LS, et al. *Lactococcus lactis* NZ9000 Prevents Asthmatic Airway Inflammation and Remodelling in Rats through the Improvement of Intestinal Barrier Function and Systemic TGF- $\beta$  Production. *Int Arch Allergy Immunol*. 2021;182(4):277–91.
  20. Wang X, Xie W, Cai L, Han C, Kuang H, Shao Y, et al. Microencapsulated *Limosilactobacillus reuteri* Encoding Lactoferricin-Lactoferrampin Targeted Intestine against *Salmonella typhimurium* Infection. *Nutrients*. 2023 Dec 18;15(24):5141.
  21. J L, X F, L L, Y Y, E M, Jc L, et al. *Limosilactobacillus reuteri* normalizes blood-brain barrier dysfunction and neurodevelopment deficits associated with prenatal exposure to lipopolysaccharide. *Gut microbes* [Internet]. 2023 Dec [cited 2024 Apr 15];15(1). Available from: <https://pubmed.ncbi.nlm.nih.gov/36799469/>
  22. Qin R, Wang J, Chao C, Yu J, Copeland L, Wang S, et al. RS5 Produced More Butyric Acid through Regulating the Microbial Community of Human Gut Microbiota. *J Agric Food Chem*. 2021 Mar 17;69(10):3209–18.
  23. Song B, Sun P, Kong L, Xiao C, Pan X, Song Z. The improvement of immunity and activation of TLR2/NF- $\kappa$ B signaling pathway by *Romboutsia ilealis* in broilers. *J Anim Sci*. 2024 Jan 3;102:skae286.
  24. Gang S, Bai W, Yu H, A G, Wang Z. *Dracocephalum moldavica* L. extract alleviates experimental colitis in rats by modulating gut microbiome and inflammatory pathways. *Mol Med Rep*. 2023 Dec;28(6):228.
  25. Mangutov EO, Alieva AA, Kharseeva GG, Voronina NA, Alekseeva LP, Evdokimova VV, et al. *Corynebacterium* spp.: relationship of pathogenic properties and antimicrobial resistance. *Klin Lab Diagn*. 2022 Sep 12;67(9):519–24.
  26. Xu J, Lu L, Jiang S, Qin Z, Huang J, Huang M, et al. Paeoniflorin ameliorates oxaliplatin-induced peripheral neuropathy via inhibiting neuroinflammation through influence on gut microbiota. *Eur J Pharmacol*. 2024 May 15;971:176516.
  27. Carroll LM, Pierneef R, Mafuna T, Magwedere K, Matle I. Genus-wide genomic characterization of *Macrocooccus*: insights into evolution, population structure, and functional potential. *Front Microbiol*. 2023;14:1181376.
  28. Miceli MH. Central Nervous System Infections Due to *Aspergillus* and Other Hyaline Molds. *J Fungi (Basel)*. 2019 Aug 30;5(3):79.
  29. Wachsmuth HR, Weninger SN, Duca FA. Role of the gut–brain axis in energy and glucose metabolism. *Exp Mol Med*. 2022 Apr 26;54(4):377–92.
  30. Mou Y, Du Y, Zhou L, Yue J, Hu X, Liu Y, et al. Gut Microbiota Interact With the Brain Through Systemic Chronic Inflammation: Implications on Neuroinflammation, Neurodegeneration, and Aging. *Front Immunol*. 2022 Apr 7;13:796288.

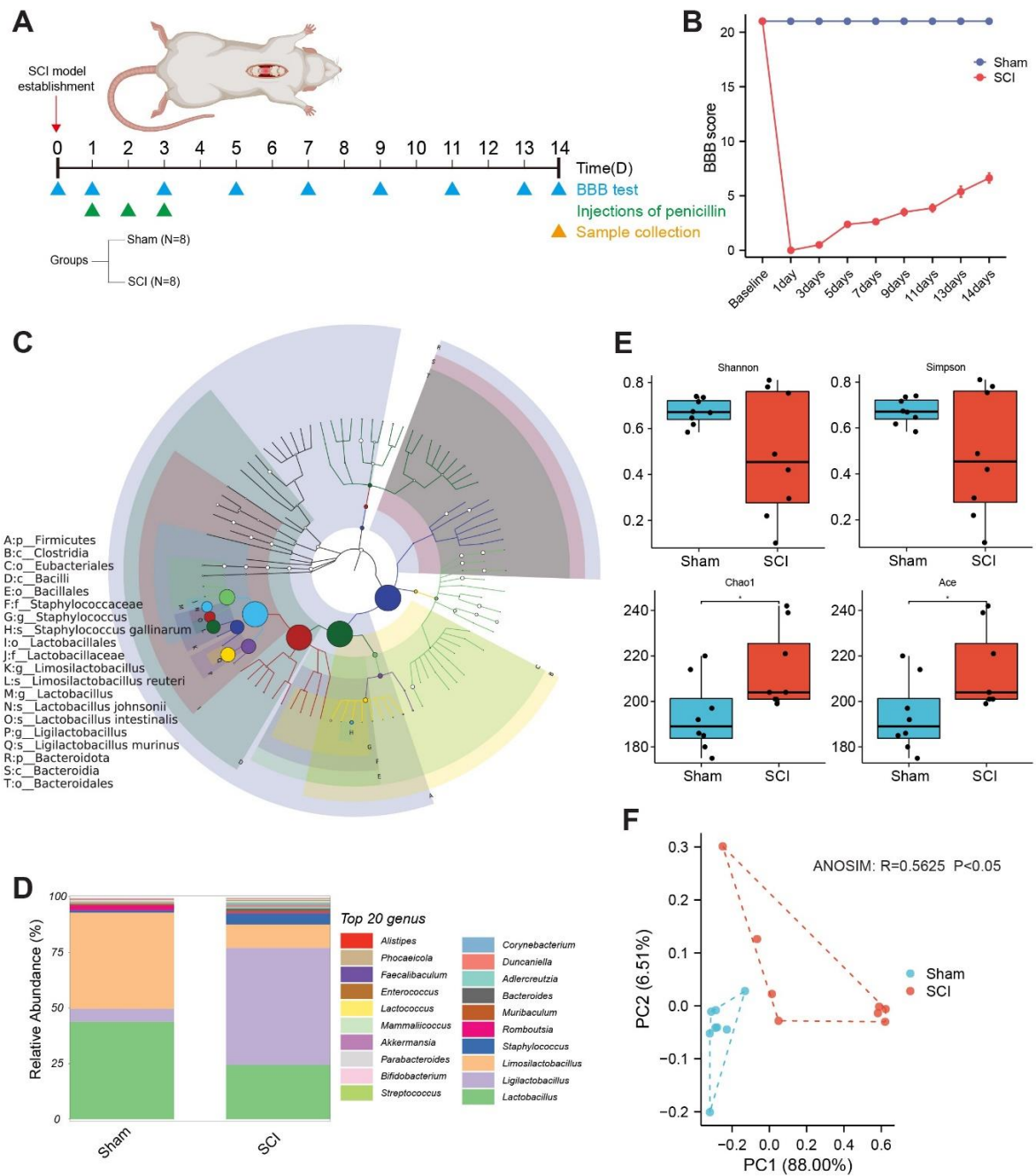
- 
31. Haupt M, Gerner ST, Bähr M, Doepfner TR. Neuroprotective Strategies for Ischemic Stroke—Future Perspectives. *IJMS*. 2023 Feb 22;24(5):4334.
  32. Schoeler M, Caesar R. Dietary lipids, gut microbiota and lipid metabolism. *Rev Endocr Metab Disord*. 2019 Dec;20(4):461–72.
  33. Islam F, Bepary S, Nafady MH, Islam MdR, Emran TB, Sultana S, et al. Polyphenols Targeting Oxidative Stress in Spinal Cord Injury: Current Status and Future Vision. *Oxid Med Cell Longev*. 2022 Aug 22;2022:8741787.
  34. Bauman WA, Spungen AM. Carbohydrate and lipid metabolism in chronic spinal cord injury. *J Spinal Cord Med*. 2001;24(4):266–77.
  35. Farkas GJ, Pitot MA, Berg AS, Gater DR. Nutritional status in chronic spinal cord injury: a systematic review and meta-analysis. *Spinal Cord*. 2019 Jan;57(1):3–17.
  36. Lanza M, Campolo M, Casili G, Filippone A, Paterniti I, Cuzzocrea S, et al. Sodium Butyrate Exerts Neuroprotective Effects in Spinal Cord Injury. *Mol Neurobiol*. 2019 Jun;56(6):3937–47.
  37. Chen H, Chen S, Zhang H, Wang S, Li Y, Meng X. N-methyl-D-aspartate receptor-mediated spinal cord ischemia-reperfusion injury and its protective mechanism. *Folia Neuropathol*. 2022;60(3):308–15.
  38. Okon EB, Streijger F, Lee JHT, Anderson LM, Russell AK, Kwon BK. Intraparenchymal Microdialysis after Acute Spinal Cord Injury Reveals Differential Metabolic Responses to Contusive versus Compressive Mechanisms of Injury. *Journal of Neurotrauma*. 2013 Sep 15;30(18):1564–76.
  39. Di Paola R, Impellizzeri D, Salinaro AT, Mazzon E, Bellia F, Cavallaro M, et al. Administration of carnosine in the treatment of acute spinal cord injury. *Biochemical Pharmacology*. 2011 Nov;82(10):1478–89.
  40. Xia C, Tian Q, Kong L, Sun X, Shi J, Zeng X, et al. Metabolomics Analysis for Nitrite Degradation by the Metabolites of *Limosilactobacillus fermentum* RC4. *Foods*. 2022 Mar 30;11(7):1009.
  41. Shi J, Che J, Sun X, Zeng X, Du Q, Guo Y, et al. Transcriptomic Responses to Nitrite Degradation by *Limosilactobacillus fermentum* RC4 and Effect of *ndh* Gene Overexpression on Nitrite Degradation. *J Agric Food Chem*. 2023 Sep 6;71(35):13156–64.
  42. Hossain TJ. Functional genomics of the lactic acid bacterium *Limosilactobacillus fermentum* LAB-1: metabolic, probiotic and biotechnological perspectives. *Heliyon*. 2022 Nov;8(11):e11412.
  43. Brown EM, Clardy J, Xavier RJ. Gut microbiome lipid metabolism and its impact on host physiology. *Cell Host & Microbe*. 2023 Feb;31(2):173–86.
  44. Aron-Wisnewsky J, Warmbrunn MV, Nieuwdorp M, Clément K. Metabolism and Metabolic Disorders and the Microbiome: The Intestinal Microbiota Associated With

---

Obesity, Lipid Metabolism, and Metabolic Health—Pathophysiology and Therapeutic Strategies. *Gastroenterology*. 2021 Jan;160(2):573–99.

45. Luo Z, Chen A, Xie A, Liu X, Jiang S, Yu R. *Limosilactobacillus reuteri* in immunomodulation: molecular mechanisms and potential applications. *Front Immunol*. 2023 Aug 9;14:1228754.
46. Vicariotto F, Malfa P, Torricelli M, Lungaro L, Caio G, De Leo V. Beneficial Effects of *Limosilactobacillus reuteri* PBS072 and *Bifidobacterium breve* BB077 on Mood Imbalance, Self-Confidence, and Breastfeeding in Women during the First Trimester Postpartum. *Nutrients*. 2023 Aug 9;15(16):3513.
47. Walden KE, Moon JM, Hagele AM, Allen LE, Gaige CJ, Krieger JM, et al. A randomized controlled trial to examine the impact of a multi-strain probiotic on self-reported indicators of depression, anxiety, mood, and associated biomarkers. *Front Nutr*. 2023;10:1219313.
48. Rezende RM, Oliveira RP, Medeiros SR, Gomes-Santos AC, Alves AC, Loli FG, et al. Hsp65-producing *Lactococcus lactis* prevents experimental autoimmune encephalomyelitis in mice by inducing CD4<sup>+</sup>LAP<sup>+</sup> regulatory T cells. *J Autoimmun*. 2013 Feb;40:45–57.
49. Gao K, Farzi A, Ke X, Yu Y, Chen C, Chen S, et al. Oral administration of *Lactococcus lactis* WHH2078 alleviates depressive and anxiety symptoms in mice with induced chronic stress. *Food Funct*. 2022 Jan 24;13(2):957–69.
50. Laroute V, Beaufrand C, Gomes P, Nouaille S, Tondereau V, Daveran-Mingot ML, et al. *Lactococcus lactis* NCDO2118 exerts visceral antinociceptive properties in rat via GABA production in the gastro-intestinal tract. *Elife*. 2022 Jun 21;11:e77100.
51. Cammarota G, Ianiro G, Kelly CR, Mullish BH, Allegretti JR, Kassam Z, et al. International consensus conference on stool banking for faecal microbiota transplantation in clinical practice. *Gut*. 2019 Dec;68(12):2111–21.
52. Aron-Wisnewsky J, Clément K, Nieuwdorp M. Fecal Microbiota Transplantation: a Future Therapeutic Option for Obesity/Diabetes? *Curr Diab Rep*. 2019 Aug;19(8):51.

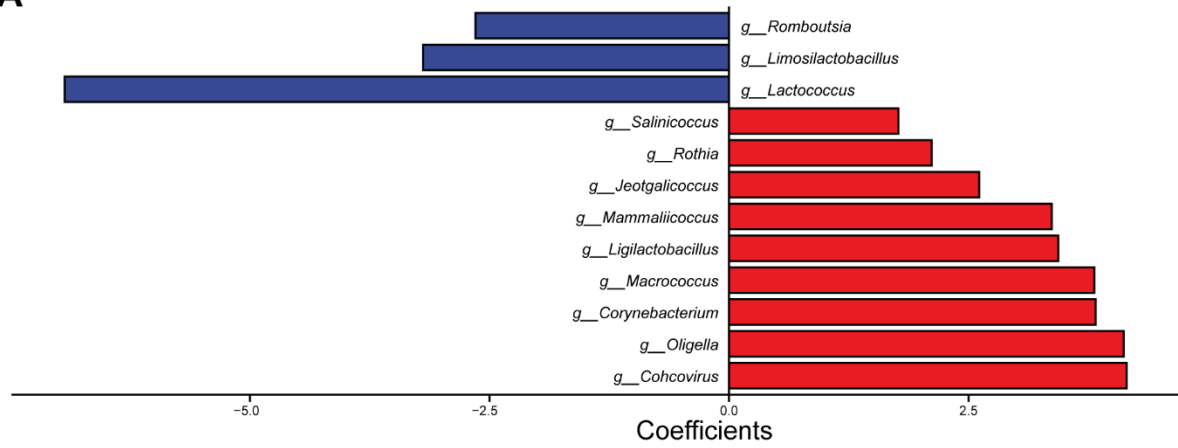
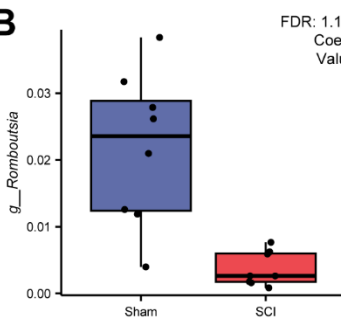
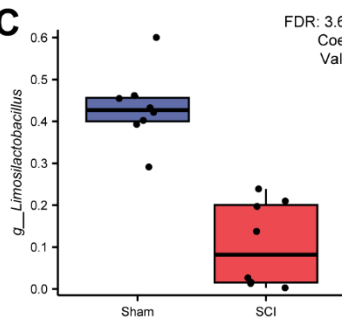
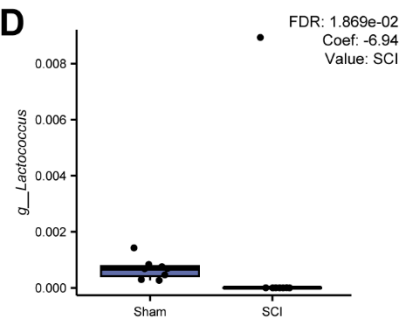
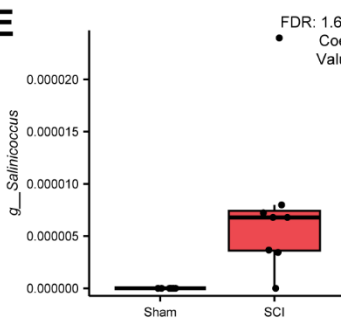
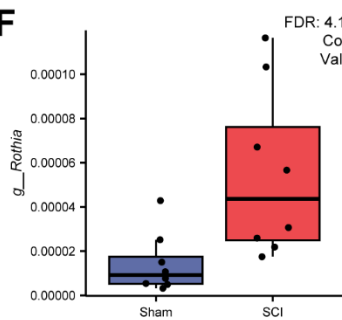
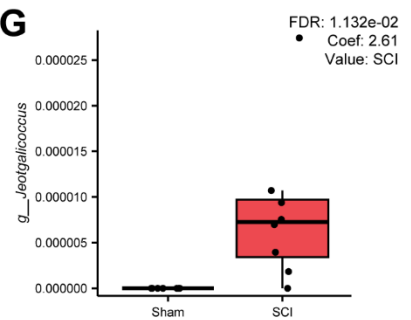
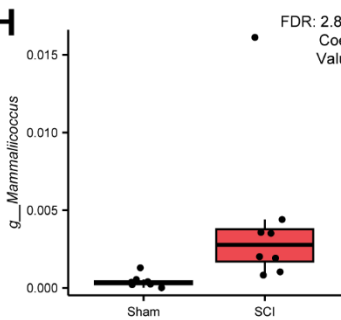
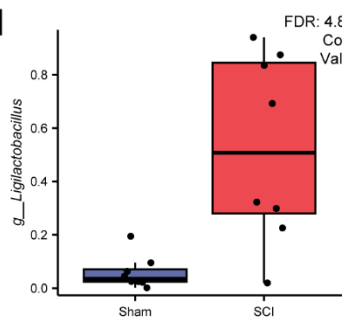
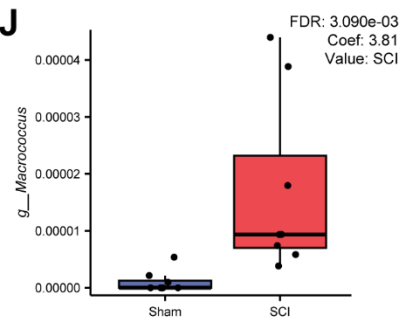
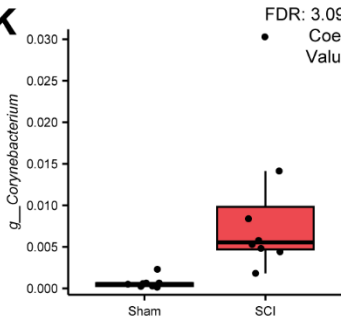
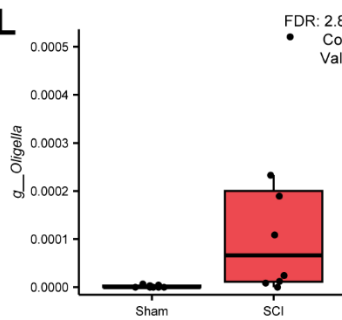
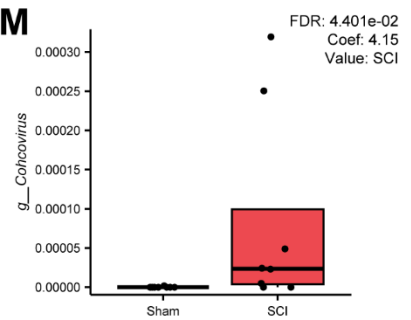
## TABLES AND FIGURES WITH LEGENDS



**Figure 1.** Impact of SCI on gut microbial composition and diversity in rats. **(A)** Schematic diagram of the experimental design, detailing the sample size and group allocation, the timeline of SCI modeling, penicillin injection, BBB testing, and sample collection. **(B)** Line chart showing the BBB scores over time. **(C)** Cladogram illustrating overall species composition, diversity, and abundance distribution. In this figure, the classification rank tree

---

from the inner circle to the outer circle shows the rank relationship of all taxa (represented by nodes) from phyla to species in the sample population, and the node size corresponds to the average relative abundance of the taxa. The top 20 taxa in the relative abundance are also identified by letters in the figure (from phyla to genus in order from outer layer to inner layer). The shadow on the letter is the same color as the corresponding node. **(D)** Stack bar plots of the top 20 dominant species at the genus level between SCI and sham groups. **(E)** Boxplots of species  $\alpha$ -diversity between the SCI group and sham group. Mann-Whitney U test,  $*P < 0.05$ . **(F)** PCoA plots showing clear clustering separation between SCI and sham groups. ANOSIM:  $R = 0.5625$ ,  $P < 0.05$ .

**A****B****C****D****E****F****G****H****I****J****K****L****M**

**Figure 2.** Key species differences of gut microbiome after SCI. **(A)** The bidirectional bar plot shows the results of the MaAsLin2 analysis (FDR < 0.05). The left side represents genera with decreased coefficients in the SCI group compared to the Sham group, while the right side represents genera with increased coefficients in the SCI group compared to the sham group. Blue bars indicate a decrease, red bars indicate an increase, and the length of the bars reflects the magnitude of the coefficient values. **(B-M)** Box plots illustrating the relative abundance of key genera identified through MaAsLin2 analysis, comparing the SCI group to the sham group. The coefficients (coef) and FDR values are indicated in the top-right corner of each plot.

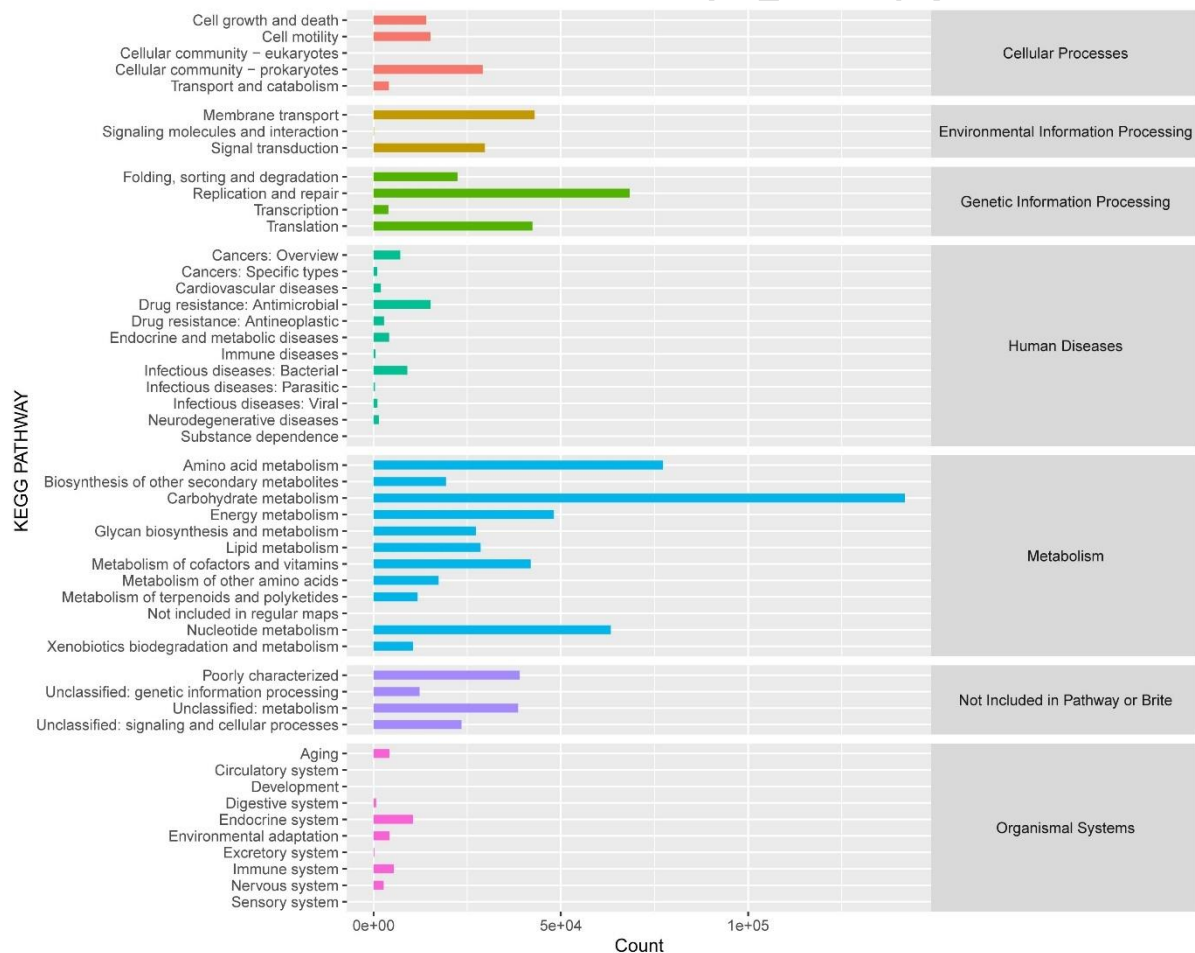


**Figure 3.** Statistical map of KEGG metabolic pathway annotation results. In the figure, the horizontal coordinate is the number of proteins annotated to the corresponding metabolic

pathway, and the vertical coordinate corresponds to each metabolic pathway of KEGG's second grade, and the classification of the first grade to which each metabolic pathway belongs is listed on the right.

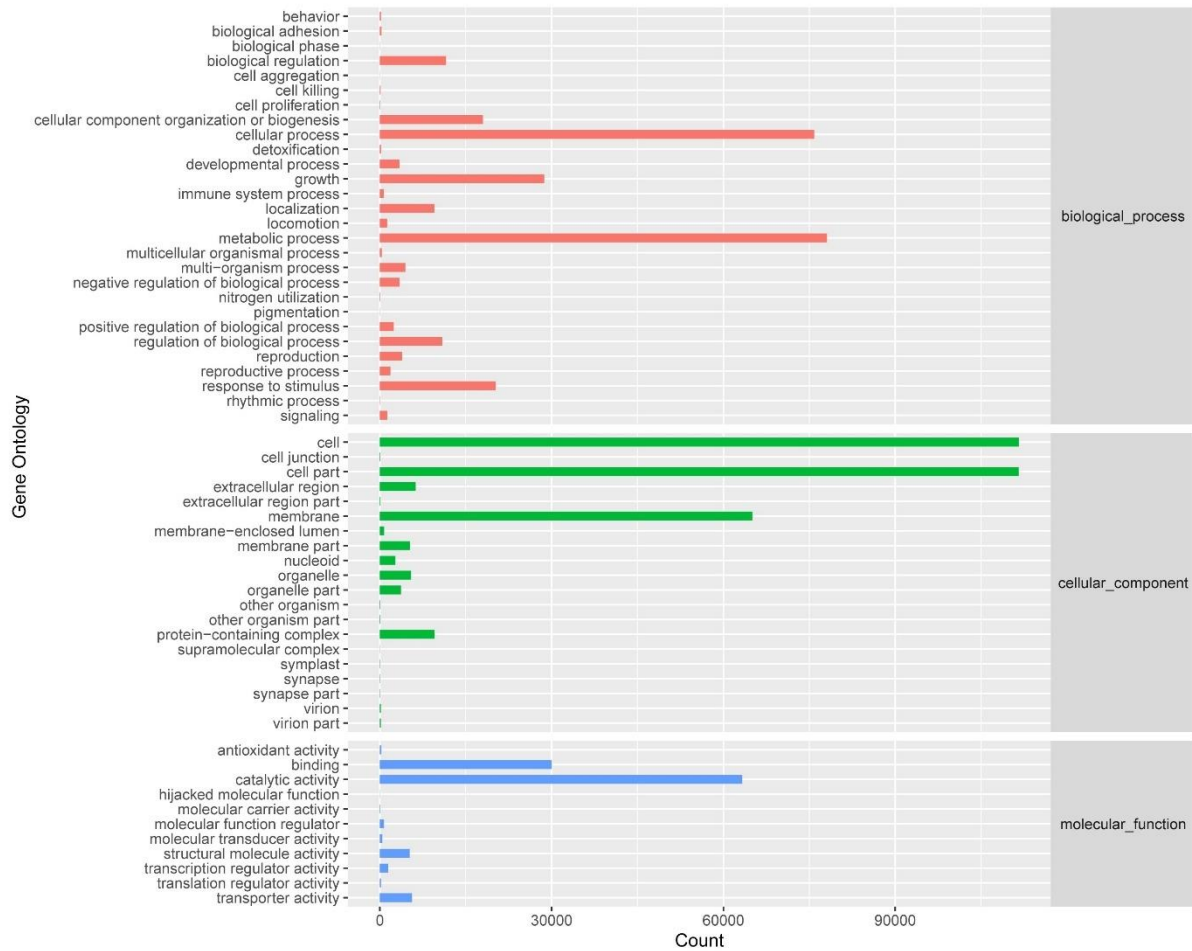
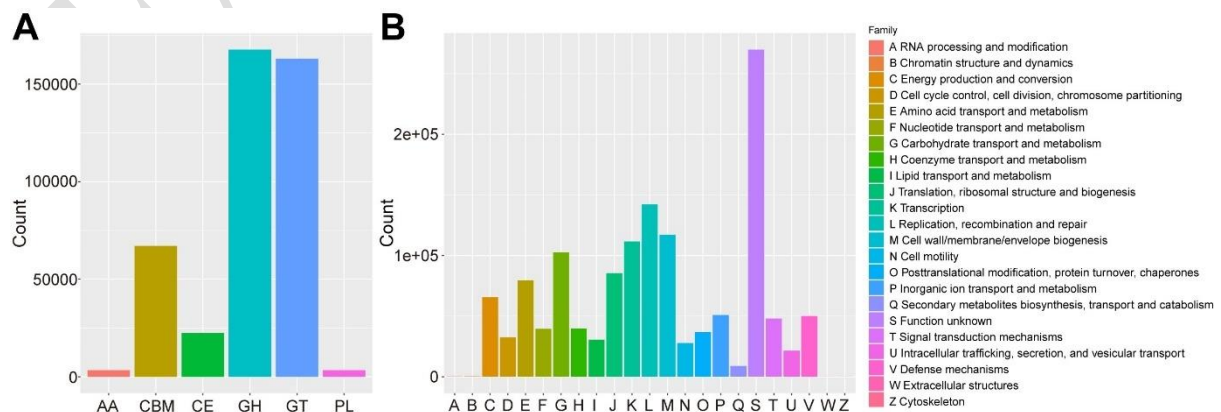
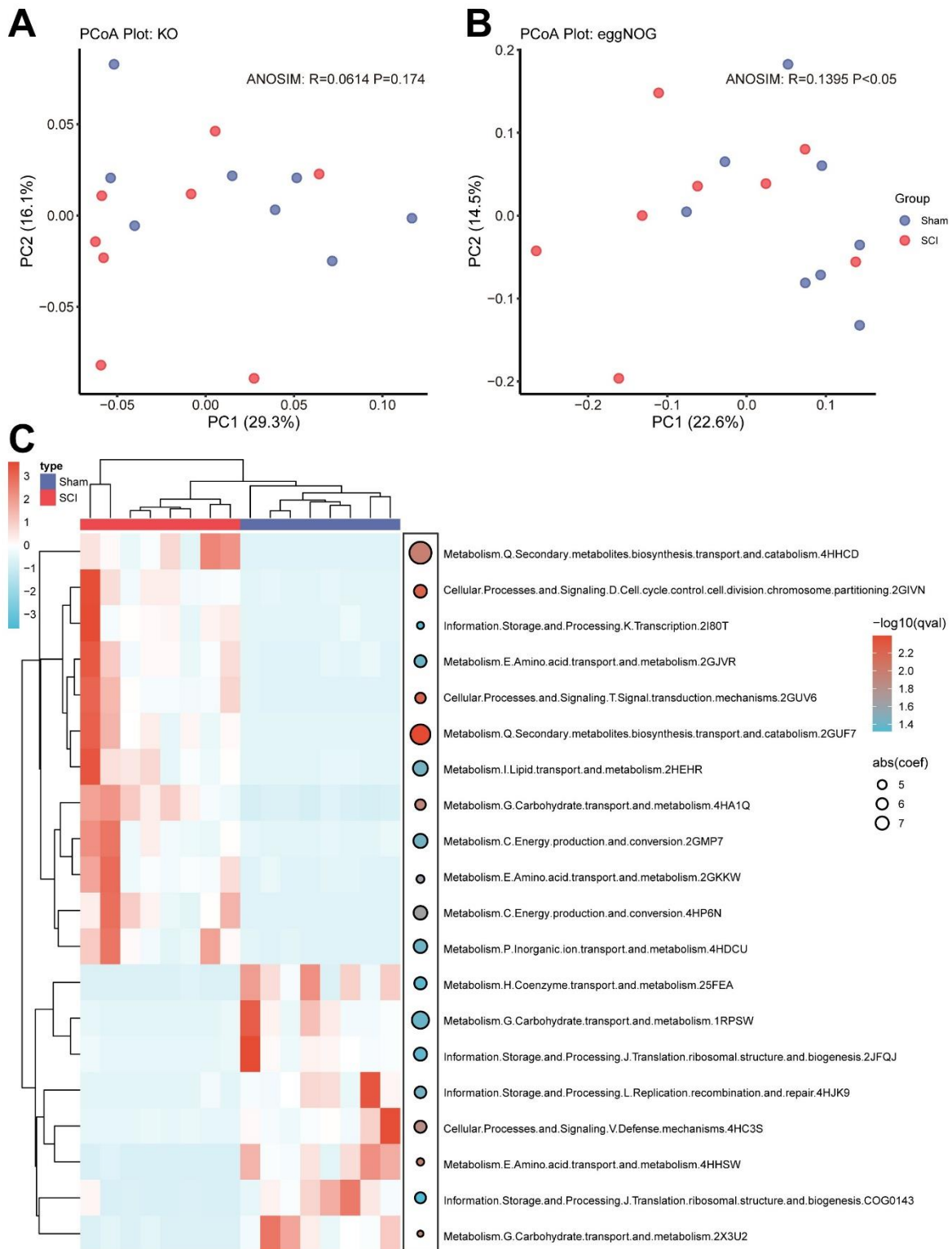


Figure 4. Statistical map of GO Slim annotation results.



---

**Figure 5.** CAZy and EggNOG annotation results. **(A)** Statistical diagram of annotation results of CAZy enzyme function module. In the figure, the horizontal coordinate corresponds to each CAZy enzyme function module, and the vertical coordinate is the number of protein families annotated to the corresponding module. Abbreviations for CAZy enzyme function modules are as follows: AA for Auxiliary Activities, CBM for Carbohydrate-Binding Modules, CE for Carbohydrate Esterases, GH for Glycoside Hydrolases, GT for Glycosyltransferases, and PL for Polysaccharide Lyases. **(B)** EggNOG function group annotation statistics. In the figure, the horizontal coordinate corresponds to the 25 functional categories of eggNOG genes, each of which is represented by an English capital letter.



**Figure 6.** Key differences in gut microbial community structure after SCI. (A) PCoA plot of functional enrichment results based on the KO database. ANOSIM:  $R = 0.0614$ ,  $P = 0.174$ . (B) PCoA plot of functional enrichment results based on the eggNOG database. ANOSIM:  $R = 0.1395$ ,  $P < 0.05$ . (C) Heatmap illustrating the coefficients and FDR of enriched pathways

identified through MaAsLin2 analysis. On the right, bubble size represents the absolute value of the coefficients, with larger bubbles indicating larger absolute values. The color of the bubbles reflects the FDR values (FDR < 0.05).

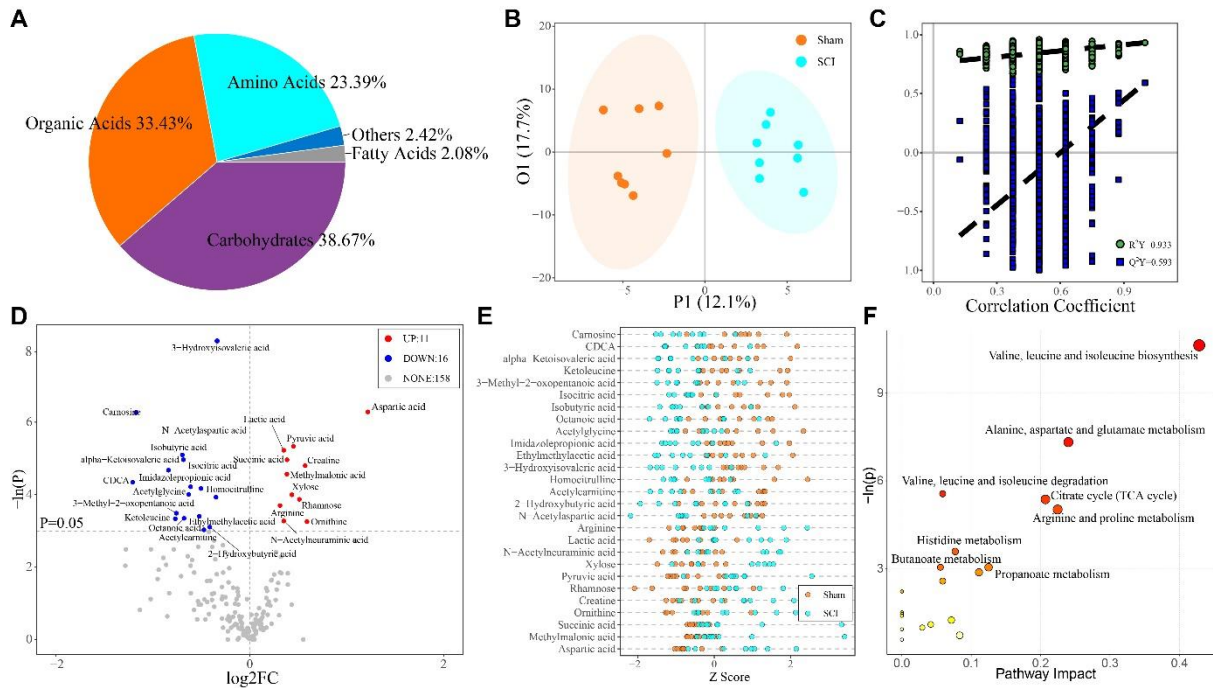


**Figure 7.** Significant Changes in Host Serum Metabolites Due to SCI. **(A)** pie plot of the proportion of identified metabolite classes in all samples. **(B)** OPLS-DA Score Plot. **(C)** Permutation Plot of OPLS-DA. **(D)** Volcano plot of Univariate Statistics.  $|\log_2FC| \geq 0$ ,  $P < 0.05$ . All metabolites were derived from  $VIP > 1$  metabolites in OPLS-DA. **(E)** Z Score dot plot of the differential metabolites. **(F)** Pathway Analysis bubble plot by rno set.  $P < 0.05$ .

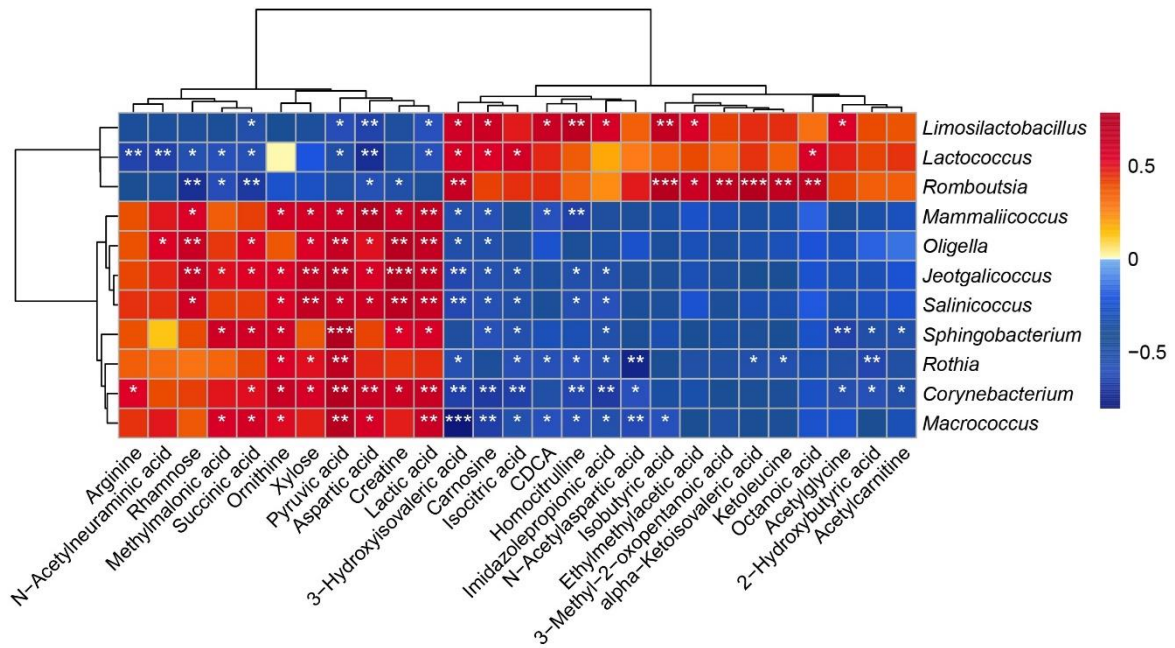


**Figure 8.** Spearman correlation heatmap between gut microbes and serum metabolites ( $R > 0.7$ ,  $*P < 0.05$ ,  $**P < 0.01$ ,  $*** P < 0.001$ ).

EARLY ACCESS